TIRE VIBRATION TRANSMISSION PART II: TEST AND MODAL MODEL QUALITY ASSESSMENT

Robert L. Wheeler, Hans R. Dorfi, Gordon H. Griffiths, and **Jeffry D. Cotton**

Tire Engineering Technology

Hankook Tire Co., Akron Technical Center

3535 Forest Lake Drive

Uniontown, OH 44685

ABSTRACT

Tire modal models are an integral part of automotive NVH vibration transmission simulations. To assess the quality of a tire modal model a correlation study has been performed on axle (spindle) responses of two dynamic load conditions, axle excitation and tire footprint excitation. A typical production tire with a static vertical load representative of a vehicle in-service condition is used. Physical testing and simulations are performed up to 150 Hz. The modal model is produced from modal parameters of a correlated FEA model, with modes calculated to 210 Hz, and measured modal damping. Forced response solutions on the dynamic loading simulations with the tire modal model are used to calculate FRF's. Measured FRF mean values and variations are established through test repetition. Correlation and model quality are assessed by using FRF based comparison metrics. The Frequency Response Assurance Criteria (FRAC) and statistical methods are used. Axle vertical and fore/aft responses at the tire assembly attachment show the best correlation.

INTRODUCTION

This paper is the second of a two paper series addressing the correlation and quality of tire modal models used in tire vibration transmission simulations. Correlation between finite element analysis (FEA) vibration modes and Experimental Modal Analysis (EMA) is addressed in the first paper [1]. Correlation of modal model forced response predictions to measured results considering test variability is presented in this paper. The modal model is based on the correlated FEA model from the first paper.

Modal modeling and testing techniques used in this study are similar to those referenced in the previous work discussed below. All simulations and physical testing are performed on a vertically loaded *non-rolling* tire. *Localized excitation within the tire footprint* of the non-rolling tire is introduced.

PREVIOUS WORK

Prior to FEA, tire vibration transmission was typically predicted using a a single degree of freedom mass-spring-damper system to represent the tire. This model allowed input of vertical motion from the road surface. With the implementation of FEA, ride analysts have introduced various types of more complex yet efficient modal based models. The modal models allow more accurate representation of specific tire designs, more accurate representation of the road input, and an expanded frequency range of analysis.

Richards, et.al., [2] introduced a tire modal model and associated modal testing in 1985. Component mode synthesis [3] techniques are used for development of the model. The model is built from a hybrid of FEA and EMA modal data. Modal stiffness, mass, and shape information are obtained from FEA. Modal damping is obtained from EMA. Boundary conditions consisted of a vertically loaded tire with a constrained interface at the road surface and an unconstrained interface at the spindle. A specialized rig is used for performing modal tests while the tire is rolling. Mode shapes are described and illustrations obtained from FEA are provided.

The ensuing use of the above tire modal model is well documented [4-9]. Richards [4] compares response simulations to a simple spring tire model illustrating extended frequency range prediction capability of the modal model. Kao, et.al. [5] uses the modal model to simulate a vehicle rolling over a bump on a drum. Multiple grid points at the tire to road interface are employed to simulate enveloping of tire over the bump. Kao also provides more insight to the modal model formulation. Correlations with test data response functions are included. Deneuvy [6] introduces a variation of the modal model using constrained spindle boundary conditions. Mode shapes obtained from FEA and from EMA are compared. Scavuzzo [7], Clayton [8], and Gunda [9] introduce enhancements to the tire modal model to account for wheel flexibility and air cavity modes. Response simulation results are compared to modal experiment results in these latter three papers.

With a focus on experimental results, Scavuzzo [10] addresses the affect of tire design and operating parameters on tire modes. One key operating parameter

is the rolling of a tire. The rolling tire data indicates resonant frequencies drop by approximately 5% compared to the same non-rolling tire.

Correlation of EMA results and Computer Aided Engineering (CAE) simulations is well documented within the structural dynamics community. Many modal vector based concepts are implemented in part 1 [1]. Frequency Response Function (FRF) based comparisons are addressed here. First, The Frequency Response Assurance Criteria (FRAC) calculation discussed by Heylen [11] is used for single FRF to single FRF comparison. Accounting for test variability is also important in correlating CAE simulations to measured data. Moeller [12] introduces the use of Chi-Square statistics to perform hypothesis tests assessing the relationship of FRF results from CAE Noise Vibration Harshness (NVH) simulations to corresponding measured data. A variation of Moeller's approach is implemented in this study and compared to the FRAC.

TIRE, RIG, AND TEST VARIABILITY

The test item is a passenger vehicle tire with two steel belts and two radial plies. The tire size is P205/70R16 and the tire is mounted on a steel wheel. The tire/wheel assembly has an inflation pressure of 300 kPa (43.5 psi) and a vertical load of 6.7 kN (1500 lb_f).

All testing was performed on a test rig setup that is illustrated in Figure 1. The primary components are an axle with tensioned bungee cords at each end of the axle that provide vertical static loading. The inflated tire & wheel assembly is attached to the center of the axle. The stiffness of the tensioned bungee cords is approximately 10% of the vertical stiffness of the tire.

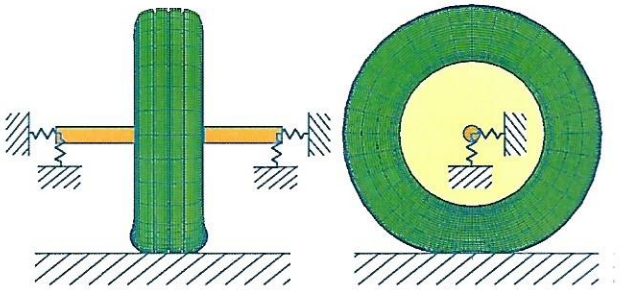

Figure 1. FEA model illustrating the tire and wheel assembly attached to rig used for modal testing.

Test variability is addressed by testing five tires obtained from the same production build of the above design. One tire was tested several times. The remaining four tires were tested once each. This sample set was used to establish measured FRF statistics. Two dynamic loading conditions are considered: Axle Dual Excitation (ADE) tests and Footprint Localized Excitation (FLE) tests.

AXLE DUAL EXCITATION (ADE) TESTS

The first dynamic loading test, the Axle Dual Excitation (ADE), was first used to perform an EMA on the tire. Measured modal data from this test was used for the tire FEA model modal vector correlation study discussed by Dorfi [1] in part one. The test was designed to excite all known tire modes in the 0-150 Hz range and to measure the appropriate responses that allow differentiation of these modes. Two reference locations were chosen on the axle. Excitation was achieved via uncorrelated burst random signals provided to electrodynamic shakers. FRF's were obtained via Multiple Input, Multiple Output (MIMO) data acquisition. Modal parameters were determined via frequency domain Multiple Degree of Freedom (MDOF) curve fitting. A total of 10 tests were performed with modal parameters extracted from each. One test was designed to obtain a good spatial description of the modes for correlation to FEA. Here 54 response locations with triaxial-translation accelerometers were measured. The other 9 tests had a reduced response location set of 29 triaxis response locations. This provided enough spatial information to permit good parameter extraction yet allowed faster test turnaround. Axle FRF's from these tests were used for the correlation study.

FOOTPRINT LOCALIZED EXCITATION (FLE) TESTS

The footprint localized excitation (FLE) test was specifically designed to provide a *local* vertical excitation within the footprint region of a non-rolling tire. It is intended to simulate road surface variations contacting a local area of the tire footprint. This is unlike testing performed by previous authors who have excited either the full footprint or have gone directly to a rolling tire that envelops over a cleat or road surface.

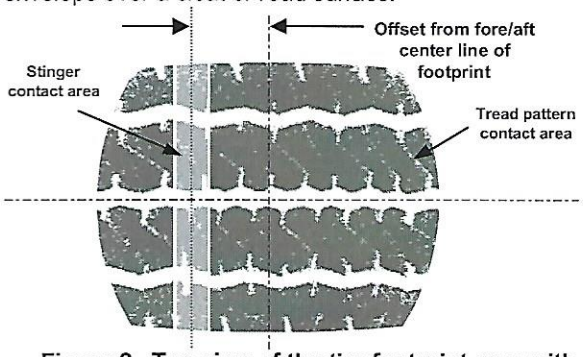

Figure 2. Top view of the tire footprint area with lighter color showing the lateral stinger contact area.

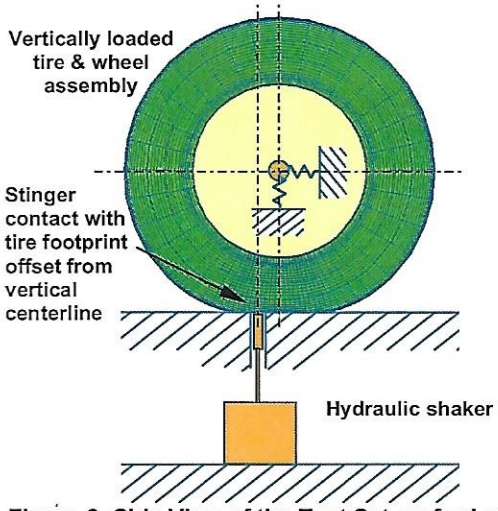

Figure 3. Side View of the Test Set-up for Local Excitation of the Tire Footprint.

To perform the FLE the test surface on which the tire is loaded was modified to allow a lateral contact area within the footprint region by a modified shaker stinger. This region is illustrated with the tire footprint image in Figure 2. The lighter shade is the area of contact by the stinger. The excitation contact area is offset from the fore/aft center of the footprint. This offset provides a moment arm intended to generate fore/aft responses in addition to vertical responses. A side view of this set-up is illustrated in Figure 3. The stinger is attached to a hydraulic shaker that provides both static preload and excitation. Random noise is used for the excitation signal. The FRF reference is the input acceleration.

EMA MEASURED DAMPING

The modal damping used in the tire modal model was obtained from modal analysis of the ADE test data. The damping results are summarized in Table 1 along with mode description and modal frequency. The table is separated into two sections: test data and tire data. The test sample data is based on one tire tested 6 times. The tire sample is based on the test sample plus 4 other tires tested once each. Mean values, standard deviations and number of samples are included. The smaller sample number for some higher frequency modes is caused by that mode not always being found by the curve fitting on some tests. The modal damping averaged 3.3% with a standard deviation of 0.2% for both the test and tire samples. The test sample mean modal frequency data was combined with mode shape data from the ADE high-response resolution test to perform the correlation with FEA results; see part 1 [1].

Table 1. EMA Modal Frequency & Damping Mean & Standard Deviations (Sigma).

Mode No.	Mode Description		Test					Tires				
			Modal Frequency (Hz)		Modal Damping (% cr)		No. Data Pts.	Modal Frequency (Hz)		Modal Damping (% cr)		No. Data Pts.
			Mean	Sigma	Mean	Sigma		Mean	Sigma	Mean	Sigma	
1	fore/aft	1	4.3	0.1	2.3	0.0	6	4.3	0.1	2.3	0.1	10
2	lateral	1	8.8	0.3	3.0	0.2	6	8.9	0.3	2.9	0.2	10
3	steer	1	18.9	0.4	3.8	0.0	6	18.9	0.4	3.7	0.2	10
4	vertical	1	22.0	0.3	4.5	0.3	6	22.1	0.6	4.5	0.3	10
5	lateral	2	36.8	0.4	2.4	0.1	6	36.9	0.9	2.3	0.2	10
6	fore/aft	2	52.8	0.4	4.1	0.1	6	52.9	1.6	4.0	0.2	10
7	lateral	3	63.2	0.5	2.8	0.1	6	63.3	1.3	2.7	0.1	10
8	lateral	4	77.7	0.5	3.0	0.1	6	77.7	1.5	2.9	0.1	10
9	steer	2	78.6	0.7	2.8	0.2	6	78.5	1.6	2.7	0.1	10
10	steer	3	92.1	0.8	3.8	0.1	6	92.1	2.1	3.7	0.1	10
11	vertical	2	96.1	0.5	3.2	1.4	6	96.3	3.1	3.4	1.1	10
12	fore/aft	3	99.7	1.4	4.6	0.5	6	99.7	3.0	4.8	0.4	10
13	fore/aft	4	102.7	0.7	3.5	0.3	6	102.7	3.2	3.4	0.3	10
14	vertical	3	111.0	0.5	3.2	0.1	6	111.2	3.4	3.2	0.1	10
15	fore/aft	5	123.4	1.3	3.2	0.1	6	123.4	3.9	3.2	0.2	10
16	lateral	5	130.9	1.2	4.1	0.2	6	130.8	3.1	4.1	0.1	10
17	vertical	4	134.4	0.9	3.0	0.2	5	134.6	4.1	3.1	0.2	9
18	wheel web	1	139.1	2.9	1.2	0.1	2	139.1	2.9	1.2	0.1	2
19	fore/aft	6	146.2	n/a	3.6	n/a	1	146.2	n/a	3.6	n/a	1
20	steer	4	146.1	1.2	4.4	0.2	4	146.1	3.1	4.5	0.3	8
	Averages			0.8	3.3	0.2			2.1	3.3	0.2	

TIRE MODAL MODEL

The tire modal model is produced from a combination of FEA & EMA data. The FEA model, which is discussed at length in part 1 [1], provides modal stiffness, mass, shape vectors, and location of spindle & footprint points. The EMA tests provide the modal damping. A schematic of how this information is used to produce the tire modal model is shown in Figure 4. At the center of the schematic are the uncoupled modal spring, mass, and damper systems for each mode. The schematic shows n modes. At the top of the schematic is the spindle, represented by a single node with six degrees of freedom (DOF) defining full spatial motion. The lines connecting the spindle to the tire modes are constraint equations that contain the spindle mode shape displacement information for each of the six DOF. The footprint is shown at the bottom. There are m footprint nodes. Each footprint node represents a lateral line in the footprint. The lines connecting the footprint nodes to the tire modes represent the constraint equations that contain the constrained footprint mode shape reaction forces.

The tire modal model in this study is based on the first 30 modes obtained from the FEA model spanning up to 210 Hz. The model damping for the first 19 modes is from the measured mean of each mode. The measured mean damping of all modes is used for the last 11 modes. For this simulation, there were 15 footprint points.

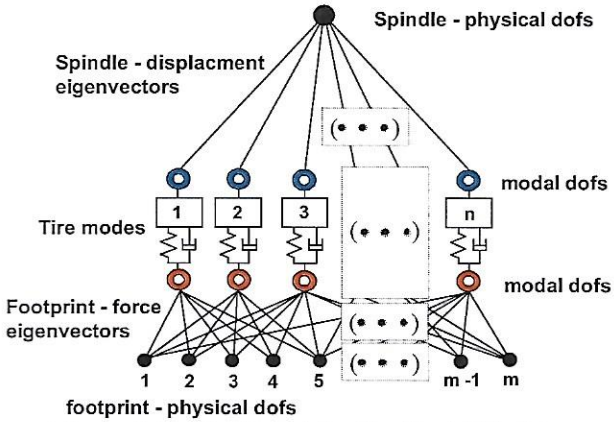

Figure 4. Illustration of the Tire Modal Model.

ADE AND FLE TEST SIMULATIONS

To perform simulations of the ADE and FLE tests, the tire modal model was connected to a simple FEA model of the test rig. The ADE test was simulated by applying a unit dynamic force to the axle in the appropriate direction at the nodes representing the locations of the shakers. All footprint nodes were constrained. The FLE test was simulated by applying a unit displacement in the vertical direction to a single footprint node at the location of the stinger. All other footprint nodes were constrained. Responses on the axle are considered for comparison since they are typically of primary interest in most vehicle simulations. More specifically the vertical and fore/aft responses at the spindle location are considered most important. This investigation also considers spindle lateral translations and 3 translations at the axle tips. The phases of the axle tip fore/aft and vertical translations provide information on rotations that may be occurring at the spindle location. The FRF's chosen for comparison are listed in Table 2.

Table 2. Compared FRF's

FRF Number	Location	Orientation
1	Axle Center	Vertical
2	Axle Center	Fore/Aft
3	Axle Center	Lateral
4	Axle Inboard	Vertical
5	Axle Outboard	Fore/Aft
6	Axle Inboard	Lateral

CORRELATION OF THE ADE SIMULATION

ADE simulation and measured FRF's from 2-150 Hz are compared. Figure 5 contains plots of the predicted FRF's overlayed on the measured mean, single standard deviation band, and peak to peak band. The responses shown, from top to bottom, are vertical, fore/aft and lateral at the axle center, vertical at the axle inboard and fore/aft at the axle outboard. Inspection of these plots shows that as a whole the model is properly simulating the measured dynamics. If the investigation were limited to the center vertical and fore/aft responses the model matches the data very well. The simulated FRF at the vertical center appears to fall within the measured single standard deviation band across much of the studied frequency range. Some of the differences may be attributed to all damping being accounted for in the model through the modal damping in the tire modal model.

Expanding observation to the other directions and locations, first the lateral center indicates that the simulation is not accurately predicting modes beginning just above 60 Hz. A peak near 80 Hz is missed or shifted at the inboard axle tip vertical response. Dorfi [1] discusses discrepancies between the FEA predicted and EMA measured modal frequencies near this frequency range and relates it to wheel flexibility not being accounted for in the base FEA model. That discrepancy may be carried through to this simulation.

Comparison metrics are considered next. The first metric is the Frequency Response Assurance Criteria (FRAC), see Heylen [11]. The FRAC is defined by the following equation,

$$FRAC(j) = \frac{\left|\left\{H(\omega_i)_j^a\right\}\cdot\left\{H(\omega_i)_j^x\right\}^*\right|^2}{\left(\left\{H(\omega_i)_j^a\right\}\left\{H(\omega_i)_j^a\right\}^*\right)\cdot\left(\left\{H(\omega_i)_j^x\right\}\left\{H(\omega_i)_j^x\right\}^*\right)} \quad (1)$$

The FRAC, like the Modal Assurance Criteria (MAC), provides a measure of the degree of alignment or parallelism between two vectors, the simulated FRF's (H^a) and the measured FRF's (H^x) in this case. However it does not indicate a difference due to global scaling or sign reversal. These are important parameters when comparing FRF's. Therefore a FRAC of 1.0 means there is correlation in the sense that the two FRF's have the same shape. A FRAC approaching zero indicates low correlation.

FRAC calculations were performed on the 6 FRF's listed in Table 2. Figure 6 contains FRAC values calculated for the simulation versus 9 measured tires. The highest FRAC values are consistently observed at the axle center vertical response (FRF 1). The lowest values are consistently observed at the inboard vertical (FRF 4). The low FRAC's

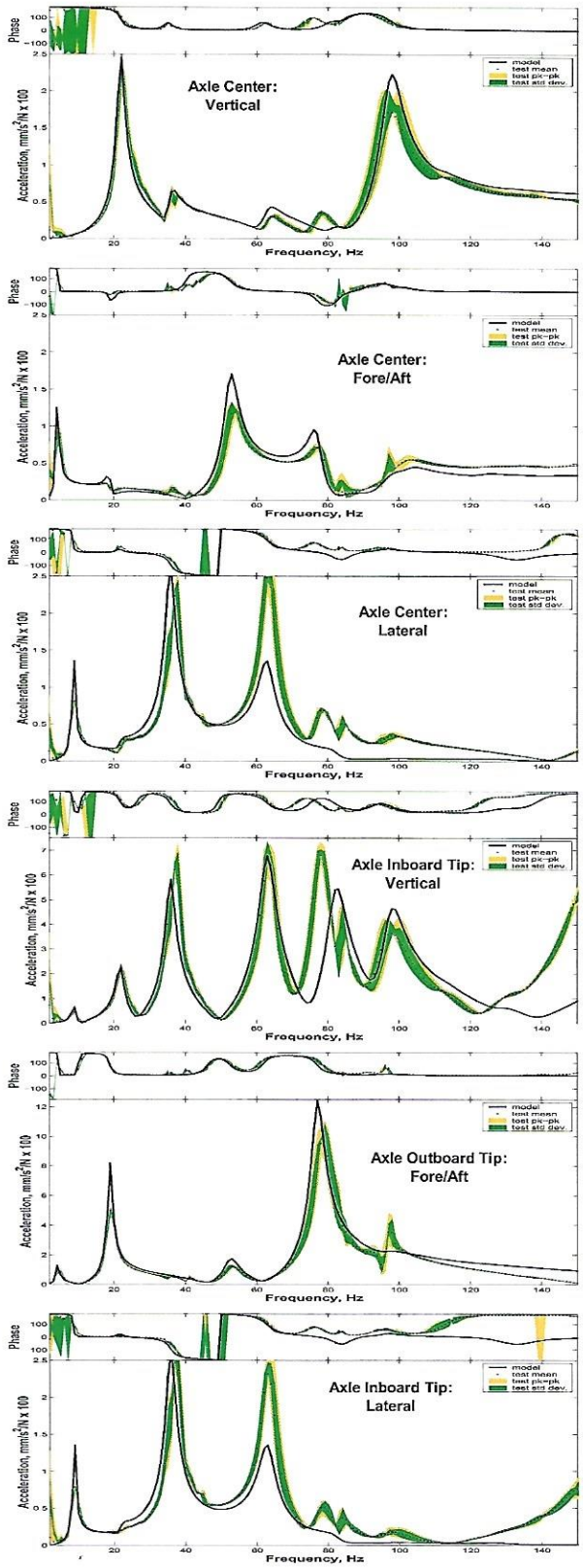

Figure 5. FRF's: ADE Simulation and Test

at this location can be attributed the 80 Hz discrepancy observed in Figure 5. It is interesting to note that a dramatic improvement occurs in the FRAC values when the calculation is limited to the 2-75 Hz range. This is illustrated in Figure 7. Notice the significant increase in the FRAC values for inboard vertical FRF's compared to those in Figure 6.

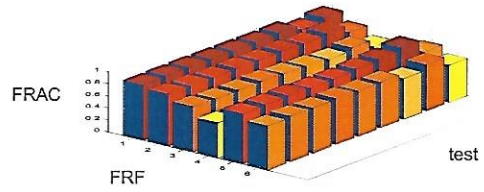

Figure 6. FRAC: ADE Simulation vs. 9 Measured Tires, for 2-150 Hz.

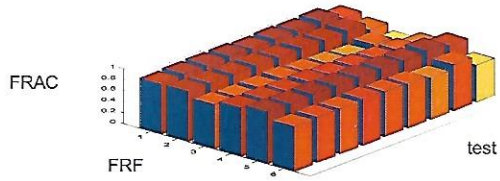

Figure 7. FRAC: ADE Simulation vs. 9 Measured Tires, for 2-75 Hz.

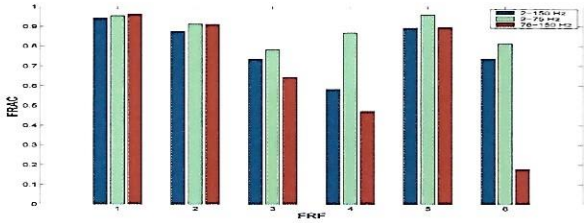

Figure 8. FRAC: ADE Simulation vs. Mean of 9 Measured Tires, for 3 Frequency Bands.

The FRAC is next compared to the mean FRF at each location for the 9 tests. Figure 8 contains a grouped bar chart showing the FRAC values at each DOF. The first bar in each group is for 2-150 Hz range, the second for 2-75 Hz, and the third for 76-150 Hz. This FRAC information indicates the best correlation occurs in the 2-75 Hz range. For the 2-150 Hz range, the FRAC values have a mean of 0.79 ± 0.13 standard deviations (σ) and a minimum of 0.58. For 2-75 Hz, the mean of the FRAC's improves to 0.88 ± 0.07 σ, with a minimum of 0.78. For 76-150 HZ, the mean of the FRAC's drops to 0.68 ± 0.31 σ, with a minimum of 0.18.

The second metric allows comparison of the FRF overall data amplitudes thus overcoming a limitation of the FRAC. It is based on the Chi-Square Test statistic, D_k, which is used by Moeller [12] for CAE NVH quality assessment and vehicle classification.

The D_k test statistic, averaged over the frequency band in consideration, is shown in the following equation,

$$\overline{D}_k = \frac{1}{J}\left(\frac{n}{n+1}\right)\left(\frac{1}{\overline{s}^2_{\bullet,\bullet,k}}\right)\sum_{j=1}^{J}\left[h^a_{j,k} - \overline{h}^x_{\bullet,j,k}\right]^2 \quad (2)$$

where,

$$\overline{s}^2_{\bullet,\bullet,k} = \frac{1}{J}\sum_{j=1}^{J} s^2_{\bullet,j,k} \quad (3)$$

$$\overline{h}^x_{\bullet,j,k} = \frac{1}{n}\sum_{i=1}^{n} h^x_{i,j,k} \quad (4)$$

$$s^2_{\bullet,j,k} = \frac{1}{n-1}\left[\left(\sum_{i=1}^{n}\left(h^x_{i,j,k}\right)^2\right) - n\left(\overline{h}^x_{\bullet,j,k}\right)^2\right] \quad (5)$$

and,

n = number of tires tested,
k = number of measured FRF's per test,
J = number of discrete frequency cells within the frequency band analyzed,
$h^x_{i,j,k}$ = amplitude of a measured FRF on tire i, at frequency j, and located at DOF k.
$h^a_{j,k}$ = amplitude of a simulated FRF at frequency j, and located at DOF k.
$s^2_{\bullet,j,k}$ = variance of measured FRF's amplitude at frequency j, and located at DOF k over n tested tires
$s^2_{\bullet,\bullet,k}$ = pooled variance; variance of measured FRF's at DOF k averaged over J frequency cells

Inspection of the terms in equation (2) shows that $\bar{D}_k$ can be also defined as the mean square error (MSE) of the simulated FRF at location k normalized with respect to the pooled variance. The first term and the last term form the MSE between the simulation FRF and the mean of the measured FRF's. Dividing the MSE by the pooled variance of the test sample FRF's provides a normalized value. Furthermore the square root of this term can be considered as a normalized difference or error, $\bar{E}_k$, with respect to the pooled standard deviation.

Instead of using D_k or $\bar{D}_k$ to perform statisitcal hypothesis testing on the FRF's like Moeller [12], $\bar{E}_k$ is used here to allow physical interpretation of the relationship between the simulation and the test data. If $\bar{E}_k$ of the simulated FRF is less than 1.0 then the model falls within the band of one standard deviation of the measured FRF's at that point. Therefore $\bar{E}_k$ values below 1.0 σ can be considered to have good correlation providing the test standard deviation is reasonable. If $\bar{E}_k$ is greater than 1.0 σ then correlation begins to drop.

$\bar{E}_k$ values were calculated for the same frequency bands as applied to the FRAC calculations above. The results are presented in Figure 9. These $\bar{E}_k$ values provide slightly different insight into the correlation. For example, the FRAC values for FRF's 1 & 2 in the 2-75 Hz range are at or above 0.9 indicating that the simulation FRF shapes correlate well with the test data. Here $\bar{E}_k$ indicates that the simulated FRF's at these same DOF's fall outside a single standard deviation of the test band. The center vertical FRF is near 1.5 σ. The center fore/aft is near 2.5 standard deviations. Overall the averaged $\bar{E}_k$ of the 6 FRF's is 2.4

σ in the 2-75 Hz range. For the full 2-150 Hz range $\bar{E}_k$ is 2.6 σ. $\bar{E}_k$ grows to 4.7 σ when calculated for the 76-150 Hz range. The Combination of the FRAC and $\bar{E}_k$ metrics replicates the above visual observations of the FRF's.

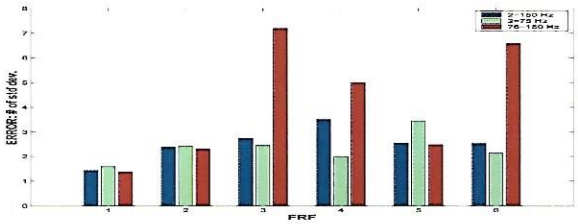

Figure 9. $\bar{E}_k$: ADE Simulation vs. Mean of 9 Measured Tires, for 3 Frequency Bands.

FLE TEST CORRELATION

The above correlation techniques were repeated for the FLE test. Simulation and measured band FRF's from the FLE test are presented in Figure 10. Two observations are made based on comparison to the ADE FRF's. First the simulation does not match the measured data in the vertical direction at the axle center as well as the ADE simulation where good correlation is apparent. Secondly, the measured standard deviation bands appear to be relatively broader than those of the ADE test. This indicates that the FLE test may not as repeatable as the EMA test.

FRAC calculations performed for the FLE simulation have different values and different trends than those produced for the ADE simulations. Figure 11 contains FLE FRAC values for the 2-150 Hz range comparing the simulation to 20 measured FRF's at the same 6 locations as analyzed above in the ADE test. Here, only the center fore/aft FRF has a consistently high FRAC for the FLE simulation.

Most FRAC values remain low for the 2-75 and 76-150 Hz bands. This is illustrated in Figure 12. Figure 13 contains FRAC values for the model compared to the *mean* of the above FRFs at each DOF. The center fore/aft FRAC remains relatively high near 0.9 over all 3 bands. The FRAC values of both axle vertical responses are higher, although still below 0.8, in the upper frequency band of 76-150 Hz as compared to the 2-75 Hz range. The above observations indicate that the model is not simulating the FLE test as well as the ADE. For the 2-150 Hz range, the FRAC values have a mean of 0.51 ± 0.13 σ which is much worse than the corresponding 0.79 ± 0.13 σ for the ALE simulation. This is further illustrated with the $\bar{E}_k$ values.

Figure 14 contains the $\bar{E}_k$ values for the FLE simulation. The first row of 6 FRAC's are for 2-150Hz, the second for 2-75 Hz, and the third for 76-150 Hz. These $\bar{E}_k$ values provide insight comparable to the FRAC values bar chart in Figure 13, i.e., the simulation has highest correlation in the fore/aft direction over the full 2-150 Hz range. Overall the averaged $\bar{E}_k$ of the 6 FRF's is 5.1 σ for the 2-150 Hz range, which is almost twice that of the ALE value of 2.6 σ.

CONCLUSIONS

A study has been performed on FRF based correlation of a tire modal model with test variability considered. The

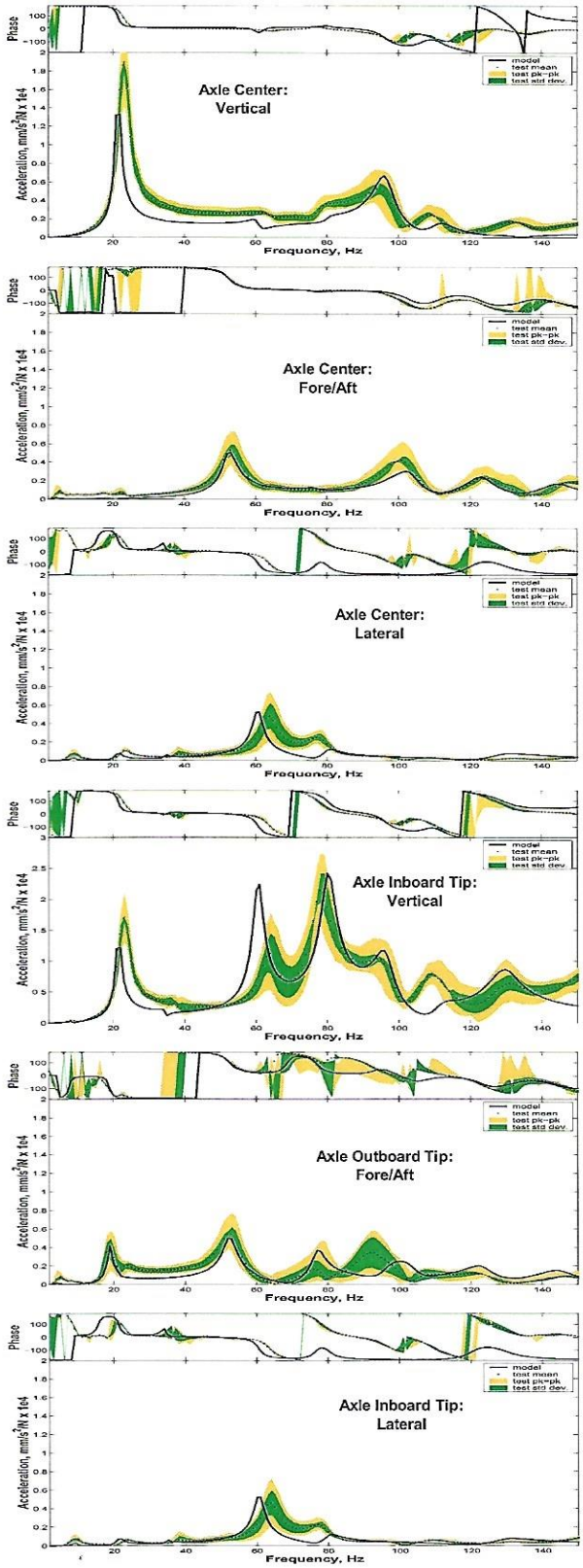

Figure 10. FRF's: FLE Simulation and Test

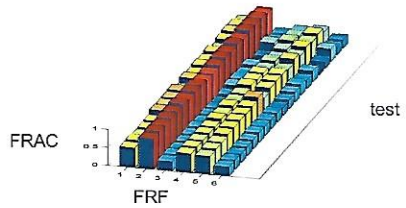

Figure 11. FRAC: FLE Simulation vs. 20 Measured Tires, for 2-150 Hz.

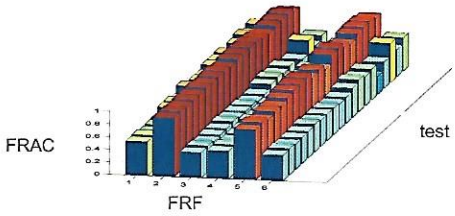

Figure 12. FRAC: FLE Simulation vs. 20 Measured Tires, for 76-150 Hz.

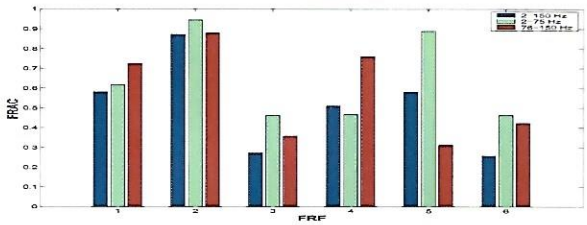

Figure 13. FRAC: FLE Simulation vs. Mean of 20 Measured Tires, for 3 Frequency Bands.

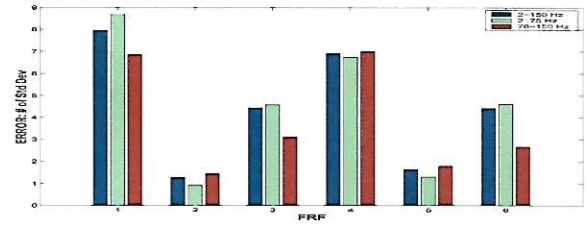

Figure 14. $\bar{E}_k$: FLE Simulation vs. Mean of 20 Measured Tires, for 3 Frequency Bands.

Frequency Response Assurance Criteria (FRAC) and a normalized error term ($\bar{E}_k$) are implemented as correlation metrics and combined to measure the overall quality of model simulations. The combined use of these metrics successfully provided objective comparisons. Furthermore applying the above calculations to frequency bands proved to be useful.

Two simulations are performed with the tire model; an axle excitation and a footprint excitation. Corresponding physical tests, including a method for local excitation within the footprint of the non-rolling tire, are described. High FRF shape correlation at the spindle location in the vertical and fore/aft directions was observed for axle excitation simulation. This was especially true in the frequency range below 75 Hz. Lower correlation was observed when more DOF's were considered and when the frequency range beyond 75 Hz to 150 Hz was considered. The modal model provided an overall low correlation when it was used to simulate local excitation of the footprint.

Future work will address improvements to the modal model to address the low correlation of the footprint excitation simulation. Full footprint excitation and local excitation at multiple positions within the footprint will be also investigated.

ACKNOWLEDGEMENTS

The support of Dr. H.J. Kim and Dr. K. Yamagishi, Hankook R&D, Taejon, Korea and R. J. Labuda and Dr. M. L. Janssen at the Hankook Tire, Akron Technical Center is acknowledged.

REFERENCES

[1] **Dorfi, H., Wheeler, R.,** and **Griffiths, G.,**. *Tire Vibration Transmission Part 1: FEA Eigensolution and Correlation,* Proceedings of the 18th IMAC , San Antonio, Texas, Feb 7-10, 2000.

[2] **Richards, T. R., Brown, J. E., Hohman, R. L., Sundaram, S. V.,** *Modal Analysis of Tires Relevant to Vehicle System Dynamics*, Proceedings of the 3rd IMAC, Orlando, FL, 1985

[3] **MacNeal, R.H.,** *A Hybrid Method of Component Mode Synthesis*, Computers & Structures Vol.1 pp.581-601, 1971.

[4] **Richards, T.R., Charek, L.T., and Scavuzzo, R. W.,** *The Effects of Spindle and Patch Boundary Conditions on Tire Vibration Modes*, SAE publication 860243, 1986.

[5] **Kao, B.G., et. al.,** *A New Tire Model for Vehicle NVH Analysis*, SAE publication 870424, 1987.

[6] **Deneuvy, A.C.,** *Modal Analysis of a Pneumatic Tyre and Dynamic Simulation by a Substructuring Method,* Proceedings of the 7th IMAC, pp. 1427-1433, Las Vegas, NV, 1989.

[7] **Scavuzzo, R. W., Charek, L.T., Sandy, P. M. and Shteinhauz, G. D.,** *Influence of Wheel Resonance on Tire Acoustic Cavity Resonance*, SAE pub. 940533, 1994.

[8] **Clayton, W.B.,** and **Saint-Cyr, R.,** *Incorporation of the Tire Air Cavity Resonance into the Modal Tire Model,* Proceedings of the 16th IMAC, pp. 50-56, Santa Barbara, California, Feb. 1998.

[9] **Gunda, R., Gau, S.,** and **Dohrmann, C.**, *Analytical Model of Tire Cavity Resonance and Coupled Tire/Cavity Modal Model,* Paper presented at the Tire Society Conference, Akron, Ohio, April 27-28, 1999.

[10] **Scavuzzo, R. W., Richards, T.R., and Charek L.T.,** *Tire Vibration Modes and Effects on Vehicle Ride Quality,* Tire Science and Technology, TSTCA, Vol. 21, No. 1, Jan-Mar, 1993, pp. 23-39

[11] **Heylen, W.,** and **Avitabile, P.,** *Correlation Considerations - Part 5 (Degree of Freedom Correlation Techniques),* Proceedings of the 16th IMAC, pp. 207-214, Santa Barbara, California, Feb. 1998.

[12] **Moeller M. J., Thomas, R.S., Chen S.E., Chandra, N., and Lenk P.,** *NVH CAE Quality Metrics*, SAE publication 1999-01-1791, 1999.